Southeast-Asian J. of Sciences: Vol. 2, No 1 (2013) pp. 87-100

PENETRATION OF CARBON NANOCYLINDER THROUGH A LIPID BILAYER

Wisit Sukchom, Kittisak Chayantrakom, Pairote Satiracoo and **Duangkamon Baowan**

Department of Mathematics, Mahidol University
Centre of Excellence in Mathematics
Bangkok 10400, Thailand
e-mail:wisitsukchom@hotmail.com; kittisak.cha@mahidol.ac.th
pairote.sat@mahidol.ac.th; daungkamon.bao@mahidol.ac.th

Abstract

Nanotechnology has brought forward new information, and innovative practices that can be utilised by applying mathematical techniques. Nanotoxicology is a branch of nanomedicine concerned with the study of toxicity of nanoparticles that may be hazardous to cells or organs. In the worst-case scenario, a tumour or cancer could possibly be induced by these nanoparticles. To study the toxicity of nanoparticles, we investigate the penetration of nanocylindrical carbon entering a lipid bilayer. We determine the interaction energy between the carbon nanocylinder and a lipid bilayer, looking at the penetration mechanism for appropriate carbon nanocylinder size. By applying the Lennard-Jones potential function and continuous approximation, the interaction energy is analysed by numerical evaluations, obtained by performing surface or volume integrals. Using this model, it has been indicated that the carbon nanocylinder with the radius and the half length of 3.55 Å will penetrate through the lipid bilayer when the hole radius of the lipid is larger than 6.65 Å. It penetrates deeper as the hole size gets larger. However, if there are no external forces, the nanoparticle will not pass the hole of the lipid bilayer but rather remains in the lipid bilayer.

Key words: carbon nanocylinder, lipid bilayer, interaction energy, Lennard-Jones potential.

1 Introduction

Living in an era of technology has opened many doors for human beings, especially in the field of nanotechnology. One of the most encouraging applications of nanotechnology is in nanomedicine; a number of researches have already been carried out in the fields of cosmetic and medical nanoparticles. Although these particles have an important role in being widely used in many industrial and consumer products but the issues of health and environmental have to be determined. Such as in the textile industry, nanoparticles create many desirable properties in the fabrics include UV blocking, stain and wrinkle resistant, flame retardant and anti-microbial, bacterial and fungal, but they might be released during the washing process. In cosmetic industry, such as the uses of nanoparticles in sun screens to block UV radiation, in emulsions to contain vitamins in facial cream and in other moisturisers to kill off bacteria. These very tiny particles may damage aquatic ecosystems when we wash off our skin and the water goes down the drain. Moreover, skin absorption or inhalation of cosmetics containing nanoparticles could cause accumulation of particles in human body and produce toxic effects due to their ability to enter cells [1, 2]. Nowadays, many researchers are worried about their side effects since there is not enough work has been done to establish the chemicals effects on human health and their safety. In this research, we determine the interaction energy between the two layers of a lipid bilayer and a carbon nanocylinder to investigate the penetration of this nanoparticle into skin.

Carbon nanocylinders or carbon nanotubes (CNT) are hollow cylinders of graphite sheets. They can be thought of as single molecules, regarding their small size with nanometer and micrometer in length or as quasi-one dimensional crystals with translation periodicity along the tube axis. This material was first observed by Endo [3], and later by Iijima [4] in the soot produced in the arc discharge synthesis of fullerenes. The unique chemical, physical and electronic properties of this particle provide the most promising avenue of research into the fabrication of nanoscale one-dimensional systems.

The lipid bilayer, made of two layers of lipid molecules, is a very thin polar membrane. It is typically about five to ten nanometers thick and surrounds all cells providing the cell membrane structure. This membrane is a flat sheet that forms a continuous barrier which acts as a permeability barrier. Natural lipid bilayers are usually composed of phospholipids, which have a hydrophilic head and two hydrophobic tails each. A schematic of a lipid bilayer is shown in Figure 1. Utilising x-ray reflectometry [5], neutron scattering [6] and nuclear magnetic resonance techniques [7], its characteristics and interactions with an aqueous environment have been studied. In 1997, Berger *et al.* [8] studied the interaction for the bilayer of dipalmitoylphosphatidylcholine (DPPC) extensively by using molecular dynamics simulations under various conditions. DPPC is a phospholipid consisting of two palmitic acids and is the major con-

stituent of pulmonary surfactant. They employed the Lennard-Jones potential function and an electrostatic term as the force field. In 2007, Qiao *et al.* [9] investigated the translocation of C_{60} fullerenes across a DPPC lipid bilayer and found that the C_{60} fullerenes could diffuse easily into the bilayer through micropores in the membrane.

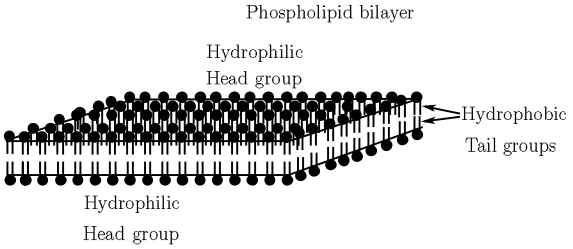

Figure 1: Schematic model of lipid bilayer.

Because of the extremely complex structure of the lipid bilayer, a coarse-grain model is adopted to study the behaviour of the lipid bilayer [10, 11, 12]. The general coarse-grain strategy involves grouping together of the selected clusters of atoms into single super-sites, to reduce the number of interaction calculations, and hence to decrease the computational cost. A typical lipid molecule, which in reality comprises more than one hundred atoms, is thus typically reduced to a collection of only a few coarse-grain sites. In 2001, Shelly *et al.* [10] used a coarse-grain model to qualitatively reproduced the density profiles of a hydrated liquid-phase dimyristoylphosphatidylcholine (DMPC) bilayer. The simulations were conducted at constant-volume and they concluded that this method is more efficient than Monte Carlo simulations to model the self-assembly of such systems. In 2004, Marrink *et al.* [11] developed a coarse-grain model for a DPPC lipid simulation which has become very popular due to its high efficiency, flexibility and simplicity. In 2011, Baowan *et al.* [13] utilised the Lennard-Jones potential function and the continuous approximation to determine the interaction between the lipid bilayer and a C_{60} fullerene using the coarse-grain model in terms of interaction energy calculations. For the system without external forces, they revealed that the C_{60} fullerene will not penetrate through the lipid bilayer but rather remains enclosed between the two layers at the mid point location.

In this paper, we utilise a coarse-grain model based on algebraic calculations using the Lennard-Jones potential as the force field. Furthermore, we investigate the feasibility of penetrating carbon nanocylinder through the lipid bilayer. The numerical results of interaction energy and consequent results for the penetration are presented. Using this model, we believe that many novel nanoscaled applications involving this nanoparticle will become apparent,

possibly impacting on therapeutic research and the construction of nanoscale systems. The paper is organised as follows; the potential function and the continuous approximation of systems are described in section 2. In section 3, penetration of carbon nanocylinder through a lipid bilayer is investigated. Numerical results and discussion of the model are presented in section 4. Finally, conclusions are given in section 5.

2 Lennard-Jones potential and Interaction energy

The non-bonded interaction energy between two molecules can be obtained by summing the potential interaction for each atom pair

$$E = \sum_i \sum_j \Phi(\rho_{ij}), \tag{1}$$

where $\Phi(\rho_{ij})$ is a potential function for atom i and j on each molecule at a distance ρ_{ij} apart. Following Girifalco *et al.* [14] and Hodak and Girifalco [15], a continuous approach is adopted where atoms are assumed to be uniformly distributed over the surfaces of the molecules. Thus, instead of the double summation shown in equation (1), the interaction energy can be obtained by performing double surface integrals, averaged over the surface of each entity

$$E = \eta_1 \eta_2 \int_{S_2} \int_{S_1} \Phi(\rho) dS_1 dS_2,$$

where η_1 and η_2 are the mean atomic surface densities of atoms on each molecule and ρ is the distance between two typical surface elements dS_1 and dS_2 on each molecule. Furthermore, the interaction energy between the atoms on the surface and atoms in the volume can be calculated by performing surface and volume integrals as follows

$$E = \eta_1 \eta_2 \int_{V_2} \int_{S_1} \Phi(\rho) dS_1 dV_2.$$

In this study, the well-known Lennard-Jones potential function [16] which is widely used in nanosystems, is employed and it is given by

$$\Phi(\rho) = -\frac{A}{\rho^6} + \frac{B}{\rho^{12}}, \tag{2}$$

where A and B are the attractive and repulsive constants, respectively. These parameters can be fitted to reproduce experimental data or accurate quantum chemistry calculations. The ρ^{-6} term describes an attraction force at long

ranges (van der Waals force or dispersion force) and the ρ^{-12} term describes the Pauli repulsion force at short ranges due to overlapping electron orbitals. Alternatively, the L-J potential (2) can be written in the form

$$\Phi(\rho) = 4\epsilon\left[-\left(\frac{\sigma}{\rho}\right)^{6} + \left(\frac{\sigma}{\rho}\right)^{12}\right],$$

where ϵ is the depth of the potential well and σ is the distance at which the inter-particle potential is zero, $\epsilon = A^2/(4B)$ and $\sigma = (B/A)^{1/6}$.

3 Penetration of the carbon nanocylinder through the lipid bilayer

We determine the interaction energy between the carbon nanocylinder of radius a and length $2L$ moving through a circular hole in a lipid bilayer as shown in Figure 2. The lipid bilayer is modeled to be located on the infinite flat plane consisting of two hydrophilic regions referred as the head group and two hydrophobic regions referred as the tail group. The head group can be represented as a flat plane whereas the tail group can be represented as a rectangular box. The distance δ between two layers of the lipid bilayer used in this investigation is taken to be 3.36 Å [13]. The Lennard-Jones constants A and B for this system are given in Table 1, where the constants for the lipid bilayer are taken from the work of Marrink *et al* [11]. For the Lennard-Jones constants of the carbon nanocylinder, we use those values of carbon nanotube which are obtained from the work of Girifalco *et al.* [14]. The constants A and B for the interaction between any two molecules are obtained from the empirical combining laws or mixing rules [17], given by $\epsilon_{12} = (\epsilon_1\epsilon_2)^{1/2}$ and $\sigma_{12} = (\sigma_1+\sigma_2)/2$, where the subscripts 1 and 2 refer to molecule 1 and 2, respectively.

Table 1: Lennard-Jones constants used in this model

Interaction	ϵ (meV)	σ (Å)	A (eV×Å^6)	B (eV×Å^{12})
CNT	2.864	3.469	19.97	3.481×10^4
Head group	18.66	4.70	804.37	8.671×10^6
Tail group	35.24	4.70	1519.37	1.638×10^7
CNT-Head group	7.31	4.085	135.87	6.314×10^5
CNT-Tail group	10.05	4.085	186.80	8.680×10^5

The mean atomic surface density of the carbon nanocylinder is taken to be 0.3812 Å^{-2} [14]. For the lipid bilayer, from the Marrink coarse-grain model [11], the head group and the tail group are coarse-grained into 2 sites and 8 sites,

respectively. Further, Bedrov *et al.* [18] employ a value of the area per lipid of 65 Å^2, and therefore, the mean atomic surface density of the head group, represented as a plane; is calculated by $\eta_{head} = 2/65 = 0.0308$ Å^{-2}. In case of the tail group, represented as a rectangular box; its mean atomic volume density is computed by $\eta_{tail} = 8/65l = 0.1231/l$ Å^{-3}, where the length l of the tail group is around 15 - 20 Å.

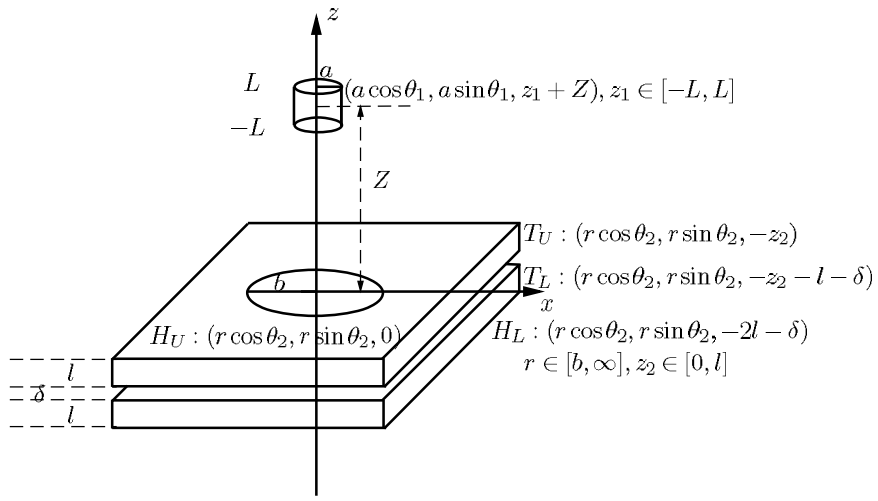

Figure 2: Schematic model of carbon nanocylinder penetrating through a hole in lipid bilayer.

In this paper, we assume that when the carbon nanocylinder interacts with the lipid bilayer, the lipid bilayer remains in equilibrium. Therefore the interaction between two layers of lipid can be neglected. So that the interaction of this mechanism composes of:

(i) The interaction between the carbon nanocylinder and the upper head group.

(ii) The interaction between the carbon nanocylinder and the upper tail group.

(iii) The interaction between the carbon nanocylinder and the lower tail group.

(iv) The interaction between the carbon nanocylinder and the lower head group.

3.1 The interaction between the carbon nanocylinder and the upper head group

With reference to a rectangular Cartesian coordinate system (x, y, z) with origin located at the centre of the hole on the upper head group, a typical point on the surface of this plane has the coordinates ($r\cos\theta_2$, $r\sin\theta_2$, 0) where $r \in (b, \infty)$ and b is the radius of the hole in the lipid bilayer. Similarly, with reference to the same rectangular Cartesian coordinate system (x, y, z), a typical point on the surface of the carbon nanocylinder has coordinates ($a\cos\theta_1$, $a\sin\theta_1$, $z_1 + Z$) where $z_1 \in (-L, L)$ and Z is the perpendicular distance in the z-direction from the surface of this plane to the centre of the carbon nanocylinder. Thus the distance ρ between two typical points on the carbon nanocylinder and the upper head group is given by

$$\begin{aligned}\rho_{h_u}^2 &= (a\cos\theta_1 - r\cos\theta_2)^2 + (a\sin\theta_1 - r\sin\theta_2)^2 + (z_1 + Z)^2 \\ &= (a-r)^2 + 4ar\sin^2[(\theta_1 - \theta_2)/2] + (z_1 + Z)^2.\end{aligned}$$

Using the Lennard-Jones potential function and the continuous approximation, the interaction energy between the carbon nanocylinder and the upper head group is given by

$$E_{h_u} = a\eta_c\eta_h \int_0^{2\pi}\int_0^{2\pi}\int_b^{\infty}\int_{-L}^{L}\left(-\frac{A}{\rho^6} + \frac{B}{\rho^{12}}\right) r\,dz_1\,dr\,d\theta_1\,d\theta_2. \qquad (3)$$

From (3), there is double integrals which can be evaluated, we define as

$$\begin{aligned}J_n &= \int_0^{2\pi}\int_0^{2\pi}\frac{1}{\rho^{2n}}d\theta_1 d\theta_2 \\ &= \int_0^{2\pi}\int_0^{2\pi}\frac{1}{[(a-r)^2 + 4ar\sin^2[(\theta_1-\theta_2)/2] + (z_1+Z)^2]^n}d\theta_1\theta_2, \qquad (4)\end{aligned}$$

where n is 3 and 6. Let $\alpha = (a-r)^2 + (z_1+Z)^2$ and $\beta = 4ar$, then (4) becomes

$$J_n = \int_0^{2\pi}\int_0^{2\pi}\frac{1}{[\alpha + \beta\sin^2[(\theta_1-\theta_2)/2]]^n}d\theta_1\theta_2. \qquad (5)$$

Equation (5) can be shown that it is independent of θ_1 or θ_2, therefore we may deduce

$$J_n = 8\pi\int_0^{\pi/2}\frac{1}{(\alpha + \beta\sin^2\phi)^n}d\phi.$$

We make the substitution $t = \cot\phi$ to obtain

$$J_n = \frac{8\pi}{(\alpha+\beta)^n}\int_0^{\infty}\frac{(1+t^2)^{n-1}}{(1+\gamma t^2)^n}dt,$$

where $\gamma = \alpha/(\alpha+\beta)$. Next we make further substitution

$$u = \frac{t}{(1+t^2)^{1/2}}, \qquad v = u^2,$$

to obtain

$$J_n = \frac{4\pi}{(\alpha+\beta)^n}\int_0^1 \frac{v^{-1/2}(1-v)^{-1/2}}{[1-(1-\gamma)v]^n}dv.$$

From Gradshteyn and Ryzhik [19](page 1005, equation 9.111), we may deduce

$$J_n = \frac{4\pi^2}{(\alpha+\beta)^n}F\left(n,\frac{1}{2};1;\frac{\beta}{\alpha+\beta}\right),$$

where $F(a,b;c;z)$ denotes a hypergeometric function. Since $F\left(n,\frac{1}{2};1;\frac{\beta}{\alpha+\beta}\right)$ admits a degenerate hypergeometric [19](page 1008, equation 9.131) so that

$$\begin{aligned} J_n = & \ \frac{4\pi^2}{(\alpha+\beta)^n}\left(\frac{\alpha}{\alpha+\beta}\right)^{\frac{1}{2}-n}F\left(1-n,\tfrac{1}{2};1;\tfrac{\beta}{\alpha+\beta}\right), \\ = & \ \frac{4\pi^2}{[(a-r)^2+(z_1+Z)^2]^{n-\frac{1}{2}}[(a+r)^2+(z_1+Z)^2]^{\frac{1}{2}}}\sum_{i=0}^{n-1}\frac{(1-n)_i(\frac{1}{2})_i}{i!^2}\left[\frac{4ar}{(a+r)^2+(z_1+Z)^2}\right]^i. \end{aligned}$$

Finally, the interaction energy defined by (3) can be rewritten as

$$E_{h_u} = a\eta_c\eta_h\left(-AI_3+BI_6\right),$$

where

$$I_n = \int_b^\infty\int_{-L}^{L} rJ_n dz_1 dr, \qquad n = 3, 6.$$

We note that the integrations with respect to θ_1 and θ_2 in the following three interactions can be evaluated in the same manner.

3.2 The interaction between the carbon nanocylinder and the upper tail group

Similar with the above system, a typical point on this region has the coordinates $(r\cos\theta_2,\ r\sin\theta_2,\ -z_2)$ where $r \in (b,\infty)$ and $z_2 \in (0,l)$, l is the length of the tail group which is chosen to be 15 Å. Consequently the distance ρ between two typical points on the carbon nanocylinder and the upper tail group is given by

$$\begin{aligned} \rho_{t_u}^2 &= (a\cos\theta_1 - r\cos\theta_2)^2 + (a\sin\theta_1 - r\sin\theta_2)^2 + ((z_1+Z)+z_2)^2 \\ &= (a-r)^2 + 4ar\sin^2[(\theta_1-\theta_2)/2] + ((z_1+Z)+z_2)^2. \end{aligned}$$

The interaction energy between the carbon nanocylinder and the upper tail group can be obtained by using the Lennard-Jones potential function and the continuous approximation, and we may deduce

$$E_{t_u} = a\eta_c\eta_t \int_0^{2\pi}\int_0^{2\pi}\int_b^{\infty}\int_0^{l}\int_{-L}^{L}\left(-\frac{A}{\rho^6}+\frac{B}{\rho^{12}}\right) r dz_1 dz_2 dr d\theta_1 d\theta_2.$$

3.3 The interaction between the carbon nanocylinder and the lower tail group

A typical point of the tail group on this region has the coordinates $(r\cos\theta_2,\ r\sin\theta_2,\ -z_2-l-\delta)$ where $r \in (b,\infty)$, $z_2 \in (0,l)$ and δ is the equilibrium separation distance between the two layers which is 3.36 Å [13]. Thus the distance ρ between two typical points on the carbon nanocylinder and the lower tail group is

$$\begin{aligned}\rho_{t_l}^2 &= (a\cos\theta_1 - r\cos\theta_2)^2 + (a\sin\theta_1 - r\sin\theta_2)^2 + ((z_1+Z)+(z_2+l+\delta))^2\\ &= (a-r)^2 + 4ar\sin^2[(\theta_1-\theta_2)/2] + ((z_1+Z)+(z_2+l+\delta))^2.\end{aligned}$$

Similarly, the interaction energy between the carbon nanocylinder and the lower tail group is given by

$$E_{t_l} = a\eta_c\eta_t \int_0^{2\pi}\int_0^{2\pi}\int_b^{\infty}\int_0^{l}\int_{-L}^{L}\left(-\frac{A}{\rho^6}+\frac{B}{\rho^{12}}\right) r dz_1 dz_2 dr d\theta_1 d\theta_2.$$

3.4 The interaction between the carbon nanocylinder and the lower head group

A typical point of the head group on this plane has the coordinates $(r\cos\theta_2,\ r\sin\theta_2,\ -2l-\delta)$ where $r \in (b,\infty)$. So that the distance ρ between two typical points on the carbon nanocylinder and the lower head group is given by

$$\begin{aligned}\rho_{h_l}^2 &= (a\cos\theta_1 - r\cos\theta_2)^2 + (a\sin\theta_1 - r\sin\theta_2)^2 + ((z_1+Z)+(2l+\delta))^2\\ &= (a-r)^2 + 4ar\sin^2[(\theta_1-\theta_2)/2] + ((z_1+Z)+(2l+\delta))^2.\end{aligned}$$

Hence, the interaction energy between the carbon nanocylinder and the lower head group is obtained as

$$E_{h_l} = a\eta_c\eta_h \int_0^{2\pi}\int_0^{2\pi}\int_b^{\infty}\int_{-L}^{L}\left(-\frac{A}{\rho^6}+\frac{B}{\rho^{12}}\right) r dz_1 dr d\theta_1 d\theta_2.$$

The total interaction energy can be obtained by combining the interaction energy for two head groups and carbon nanocylinder, and the interaction energy for two tail groups and carbon nanocylinder so that E_{total} becomes

$$E_{total} = E_{h_u} + E_{t_u} + E_{t_l} + E_{h_l}. \tag{6}$$

4 Numerical Results and Discussion

The numerical results for the interaction between a carbon nanotube and lipid bilayer are presented in Figures 3 and 4. The algebraic computer package MAPLE is utilised throughout this investigation to determine numerical solutions of the model. Figures 3 and 4 show the relation between the interaction energy and the perpendicular distance Z for various radii b of the hole in the lipid bilayer.

From Figure 3, when the radius of the hole is in the range of 0 - 3 Å, it seems that the carbon nanocylinder does not move closer to the hole of the lipid bilayer because its size is larger than the hole size. In the range of 4 - 6 Å, although the carbon nanocylinder moves closer to the hole of the lipid bilayer but when it passes the point of the minimum interaction energy, the nanoparticle will not penetrate to the hole. This is because of a much larger repulsive force than attractive force between two molecules.

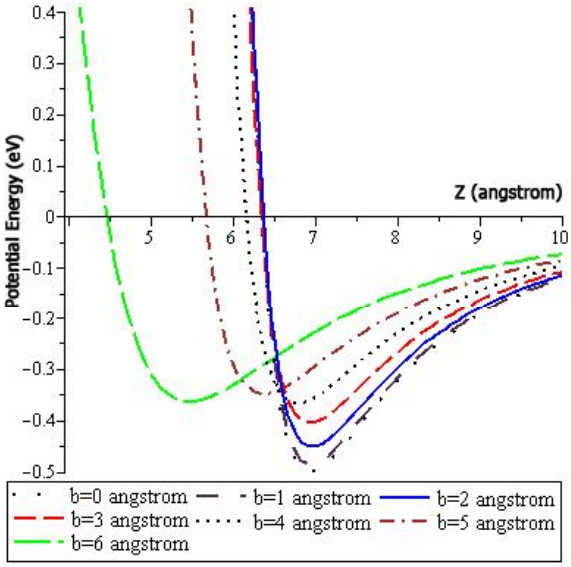

Figure 3: Potential energy profiles for carbon nanocylinder with radius $a = 3.55$ Å and half length $L = 3.55$ Å penetrating through the hole of radii $b = 0$,1 ,2 ,3 ,4 ,5 ,6 Å.

From Figure 4, the carbon nanocylinder penetrates through the hole of the lipid bilayer when the radius of the hole is larger than 7 Å. When we increase the hole size, the value of the interaction energy is also increased that means the possibility of the nanoparticle to penetrate through the lipid bilayer is

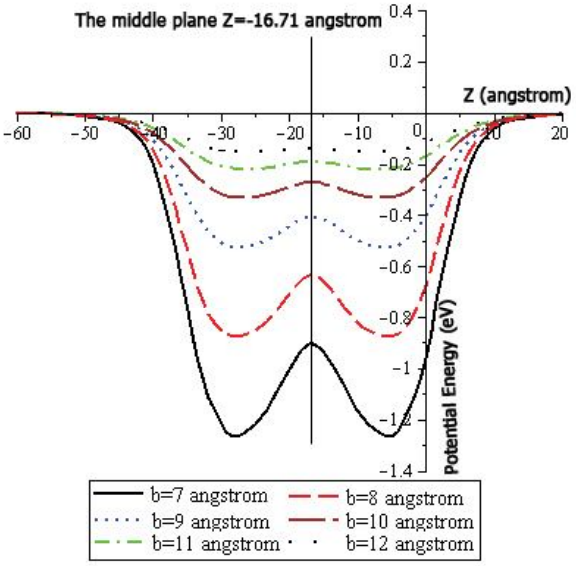

Figure 4: Potential energy profiles for carbon nanocylinder with radius $a = 3.55$ Å and half length $L = 3.55$ Å penetrating through the hole of radii $b = 7$,8 ,9 ,10 ,11 ,12 Å.

decreased. Moreover, we notice that there are two minimum energy locations, it occurs because of the symmetry structure of the lipid bilayer. Due to the symmetry of the energy profile, we can estimate the middle plane of the lipid bilayer which is around -16.71 Å from the upper head group, where the exact value which can be calculated by $Z = -l - \delta/2$ is obtained is -16.68 Å from the upper head group. The negative sign indicates the level located below the plane $z = 0$.

In Figure 5, we present the relation between the radius b of the hole and the perpendicular distance Z_{min} at the minimum interaction energy. For a positive Z_{min}, the carbon nanocylinder is located above the hole of the lipid bilayer whereas it penetrates through the hole of the lipid bilayer for a negative Z_{min}. Regarding to the penetration behaviour as shown in Figure 5, the value of Z_{min} is zero when $b = b_0 = 6.65$ Å which is the hole radius at which the centre of the carbon nanocylinder located at the origin. The nanoparticle begins to penetrate into the hole of the lipid bilayer when $b > 6.65$ Å, and it penetrates deeper as the hole radius is getting larger. However, the nanoparticle cannot pass the middle plane of the lipid bilayer. When the hole radius $b > 18.33$ Å, the nanoparticle can penetrate to the middle of the lipid bilayer and remains on that plane, we denote this value as b_m. Furthermore, we compare the results

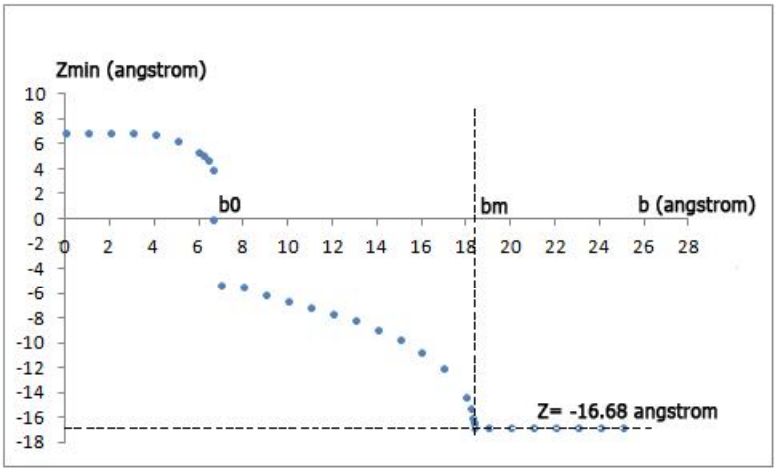

Figure 5: Relation between the perpendicular distance between the carbon nanocylinder and the hole of lipid bilayer at the minimum energy versus the hole radius of the lipid bilayer.

between the penetration of the C_{60} fullerene through the lipid bilayer [13], and this model. We find that they are not much different in the sense of behaviour, and some critical values are shown in Table 2.

Table 2: Comparison of the critical hole radii between penetration of C_{60} and that of CNT through the lipid bilayer

Interaction	b_0 (Å)	b_m (Å)
C_{60} fullerene-Lipid bilayer	6.81	17.96
CNT-Lipid bilayer	6.65	18.33

5 Conclusions

In this paper, we utilise mathematical modelling to determine the behaviour of the carbon nanocylinder or carbon nanotube (CNT) penetrating through the hole of the lipid bilayer. Elementary mechanical technique has been employed to formulate analytical expressions for this system. We consider the penetration scenario for the carbon nanocylinder where the radius and the half length are chosen to be 3.55 Å entering into the hole of the lipid bilayer, using various hole sizes in the range of 0 - 12 Å. We employ the classical Lennard-Jones potential function and the continuous approximation to determine the potential energy

which may be expressed in terms of the hypergeometric functions. Because of the complicated analytical expressions, we use the algebraic computer package MAPLE to perform numerical evaluations for our system.

We also assume that the lipid bilayer is in equilibrium when the carbon nanocylinder penetrates through the hole, so that there are only the interaction scenarios between the nanoparticles and the two layers of lipid. In the sense of interaction energy, we find that the nanoparticle will not move closer to the hole of the lipid when the hole radius is smaller than 3 Å. We presume that it occurs because of its larger size. When we increase the hole size, the nanoparticle moves closer to the hole but does not penetrate through the hole because of the larger repulsive force between them. The carbon nanocylinder will penetrate through the hole of the lipid bilayer when the hole radius is greater than 6.65 Å. The nanoparticle penetrates deeper into the lipid but it cannot move to the other side of the bilayer. Besides, we find that it rather remains in the middle plane of the lipid bilayer when the hole radius is larger than 18.33 Å.

Acknowledgements

The authors gratefully thank the Nanomechanics Group at the University of Adelaide, Australia. This paper is funded by the Centre of Excellence in Mathematics, Thailand, and this financial support is gratefully acknowledged.

References

[1] T. Thomas, K. Thomas, N. Sadrieh, N. Savage, P. Adair and R. Bronaugh, *Research Strategies for Safety Evaluation of Nanomaterials Part VII: Evaluating Consumer Exposure to Nanoscale Materials*, Toxicol. Sci. 91 (2006) 14-19.

[2] A. Nel, T. Xia, L. Madler and N. Li, *Toxic Potential of Materials at the Nanolevel*, Sci. 311 (2006), 622-627.

[3] M. Endo, *Mecanism de Croissance en Phase Vapeur de Fibres de Carbone*, PhD thesis, University of Orleans, France.

[4] S. Iijima and T. Ichihashi, *Single Shell Carbon Nanotubes of One Nanometer*, Nature 363 (1993), 603-605.

[5] B.A. Lewis and D. M. Engelman, *Lipid Bilayer Thickness Varies Linearly with Acyl Chain Length in Fluid Phosphatidylcholine Vescicles*, J. Mol. Biol. 162 (1983), 211-217.

[6] G. Zaccai, J.K. Blasie and B.P. Shoenborn, *Neutron Diffraction Studies on the Location of Water in Lecithin Bilayer Model Membranes*, Proc. Natl. Acad. Sci. USA 71 (1975), 376-380.

[7] J.L. Browning and J. Seelig, *Bilayers of Phosphatidylserine: a Deuterium and Phosphorus Nuclear Magnetic Resonance Study*, Biochem. 19 (1980), 1262-1270.

[8] O. Berger, O. Edholm and F. Jahnig, *Molecular Dynamics Simulations of a Fluid Bilayer of Dipalmitoylphosphatidylcholine at Full Hydration, Constant Pressure and Constant Temperature*, J. Biophys. 72 (1997), 2002-2013.

[9] R. Qiao, A.P. Roberts, A.S. Mount, S.J. Klaine and P.C. Ke, *Translocation of C_{60} and its Derivatives across a Lipid Bilayer*, Nano. Lett. 7 (2007), 614-619.

[10] J. C. Shelley, M.Y. Shelly, R.C. Reeder, S. Bandyopadhyay, P.B. Moore and M.L. Klein, *Simulations of Phospholipids Using a Coarse Grain Model*, J. Phys. Chem. B. 105 (2001), 9785-9792.

[11] S.J. Marrink, A.H. de Vries and A.E. Mark, *Coarse Grained Model for Semiquantitative Lipid Simulations*, J. Phys. Chem. B. 108 (2004), 750-760.

[12] R. DeVane, A. Jusufi, W. Shinoda, C.C. Chiu, S.O. Nielsen, P.B. Moore and M.L. Klein, *Parametrization and Application of a Coarse Grained Force Field for Benzene/Fullerene Interactions with Lipids*, J. Phys. Chem. B. 114 (2010), 16364-16372.

[13] D. Baowan, B.J. Cox and J.M. Hill, *Instability of C_{60} Fullerene Interacting with Lipid Bilayer*, J. Mol. Model 18 (2012), 548-557.

[14] L.A. Girifalco, M. Hodak and R.S. Lee, *Carbon Nanotubes, Buckyballs, Ropes, and a Universal Graphitic Potential*, Phys. Rev. B 62 (2000), 13104-13110.

[15] M. Hodak and L.A. Girifalco, *Fullerenes inside Carbon Nanotubes and Multi-walled Carbon Nanotubes: Optimum and Maximum Sizes*, Chem. Phys. Lett. 350 (2001), 405-411.

[16] J.E. Lennard-Jones, *Proceedings of the Physical Society*, 43 (1931), 461-482.

[17] J.O. Hirschfelder, C.F. Curtiss and R.B. Bird, *Molecular Theory of Gases and Liquids*, Wiley, Newyork (1954)

[18] D. Bedrov, G.D. Smith, H. Davande and L. Li, *Passive Transport of C_{60} Fullerenes through a Lipid Membrane: a Molecular Dynamics Simulation Study*, J. Phys. Chem. B. 112 (2008), 2078-2084.

[19] I.S. Gradshteyn and I.M. Ryzhik, *Table of Integrals, Series and Produts*, 7th edition, Academic Press (2000).